Direct Numerical Simulation of the Shock Wave Boundary Layer Interaction (SWBLI)

I. BEN HASSAN SAÏDI[a], C. TENAUD[a], G. FOURNIER[b]

a. LIMSI, CNRS, Université Paris-Saclay, Orsay, FRANCE. iben@limsi.fr ; christian.tenaud@limsi.fr
b. LMEE, Univ. Evry, Université Paris-Saclay, 91020, Evry, France. guillaume.fournier@ufrst.univ-evry.fr

Résumé :

L'objet de cet article est la simulation numérique directe de l'interaction onde de choc couche limite (IOCCL) sur une plaque plane. Lors de ce type d'interactions, l'ensemble formé par la bulle de recirculation et le système d'ondes de choc est connu pour être soumis à une oscillation longitudinale à basse fréquence. Bien que ce phénomène soit bien connu, il n'existe pas de consensus concernant le mécanisme d'apparition de cette instationnarité. Certains auteurs soupçonnent les grandes structures de la couche limite incidente d'exciter la zone s'interaction onde de choc couche limite à suffisamment basse fréquence pour déclencher l'instationnarité. D'autres auteurs soupçonnent que le mécanisme d'apparition de l'instationnarité soit plutôt dû à la dynamique de la zone de recirculation. Un code de simulation DNS/LES, parallèle (MPI), développé au LIMSI sur la base d'un shcéma volumes finis d'ordre élevé à capture de choc est utilisé pour étudier ce phénomène. Une DNS de l'interaction entre une onde de choc incidente et une couche limite laminaire est effectuée en premier lieu. En effet, dans cette configuration, une éventuelle instationnarité ne peut en aucun cas être due à la présence de structures turbulentes dans la couche limite. Dans cette configuration, l'instationnarité de l'IOCCL n'a pas été observée. Seule l'instationnarité du point de recollement a été observée. Ce résultat tend à confirmer l'importance du caractère turbulent de la couche limite incidente dans le mécanisme d'apparition de l'instationnarité de l'IOCCL. Des conditions d'entrée instationnaires (Synthetic Eddy Method adaptée pour une couche limite compressible) ont donc été développées afin de simuler une couche limite compressible turbulente sans assumer le coût prohibitif du calcul de la transition laminaire turbulent de la couche limite. Ces conditions d'entrée sont utilisées pour effectuer la simulation de l'IOCCL avec une couche limite turbulente. Cette simulation a permis de reproduire l'instationnarité du point de recollement mais également l'instationnarité du point de séparation. L'instationnarité de l'IOCCL a donc été reproduite dans cette simulation.

Abstract :

The aim of this paper is the direct numerical simulation of the shock wave boundary layer interaction (SWBLI). For these interactions, the separation bubble bubble, as well as the subsequent reflected shock wave, are known to oscillate in a low-frequency streamwise motion. The origin of those oscillations, however still unclear, has been related either to the shedding of vortices in

the mixing layer downstream of the separation, or to the turbulent structures in the incoming boundary layer. An in-house parallel (MPI) Finite-Volume DNS/LES solver base on a high order finite volume scheme with shock capturing procedure is used to study this phenomenon. As a first step, by simulating the interaction between a laminar boundary layer and an incident shock wave, we suppress the suspected influence of the large turbulent structures of the boundary layer on the SWBLI unsteadiness. In this configuration, no unsteadiness of the SWBLI has been observed. Only the unsteadiness of the reattachement point have been observed. This result tends to suggest the importance of the turbulent structures of the incoming boundary layer in the low frequency oscillations of the SWBLI system. A Synthetic Eddy Method that we adapted to compressible flow, have been developed to achieve this objective without prohibitive additional computational costs. The Synthetic Eddy Method is used to perform the DNS of a shock wave turbulent boundary layer interaction. This simulation allowed to observe the unsteadiness of the reattachement point but also of the separation point. The unsteadiness of the the whole SWBLI system has then been reproduced in this simulation.

Mots clefs : Direct numerical simulation ; turbulent flows ; compressible flows ; shock wave boundary layer interaction ; synthetic turbulent inlet conditions

1 Introduction

Situations where an incident shock wave impinges upon a boundary layer are common in the aeronautical and spatial industries. For instance, it can occur in the flow around supersonic aircrafts, in turbojets, supersonic air intakes or rocket nozzles. Under certain circumstances (High Mach number, large shock angle...), the interaction between an incident shock wave impinging a boundary layer may create an unsteady separation bubble. This bubble, as well as the subsequent reflected shock wave, are known to oscillate in a low-frequency streamwise motion that can spread over several tenth of the boundary layer thickness. This unsteadiness of the SWBLI subjects structures to oscillating loads that can lead to damages for the solid structure integrity. So, a careful attention must be paid for this issue. The origin of those oscillations, however still unclear [1], has been related either to the shedding of vortices in the mixing layer downstream of the separation [8, 7], or to the turbulent structures in the incoming boundary layer[6].

An in-house parallel (MPI) Finite-Volume DNS/LES solver is used to perform direct numerical simulations of the SWBLI in order to better understand the mechanisms leading to the unsteadiness of the SWBLI. We chose to perform SWBLI simulations suppressing one of the two suspected mechanisms leading to the unsteadiness. As a first step, by simulating the interaction between a laminar boundary layer and an incident shock wave, we suppress the suspected influence of the large turbulent structures of the incoming boundary layer on the SWBLI unsteadiness. The only remaining suspected cause of unsteadiness would be the dynamics of the separation bubble. The flow conditions are nearly similar to the test case of Degrez [5] with a shock wave angle increased in order to strengthen the interaction and trigger the unsteadiness of the separation bubble. First results [3] have shown that the location of the reattachment point

of the recirculation bubble has an oscillatory motion. A strong intermittency of the shedding responsible for low-frequency reattachment shock oscillations has also been identified. Nevertheless, in this configuration, the separation point of the recirculation bubble has a fixed location along the flat plate. Consequently, even if the recirculation bubble have an unsteady dynamics, no unsteadiness of the whole SWBLI system has however been recorded for this interaction with a laminar boundary layer. These results tend to suggest the importance of the turbulent structures of the incoming boundary layer in the low frequency oscillations of the SWBLI system. In this context, the accurate simulation of a turbulent compressible incoming boundary layer seems to be of great importance. A Synthetic Eddy Method [4] that we adapted to compressible flows, has been developed to achieve this objective without prohibitive additional computational costs. This method is used in order to perform the DNS of the shock wave turbulent boundary layer interaction.

In a first section, the equations and the numerical scheme used in this study will be presented. In a second section, results on the simulation of the unsteady interaction between an incident shock wave and a laminar boundary layer will be presented. The last section tackles the simulation of an oblique shock wave interacting with a turbulent boundary layer using the Synthetic Eddy Method for generating adequate inlet turbulent boundary conditions.

2 Numerical methods.

We consider the compressible Navier-Stokes equations. The simulations are performed with an in-house parallel (MPI) Finite-Volume based DNS/LES solver developed at LIMSI-CNRS. The convective fluxes are discretized by Monotonicity-Preserving shock-capturing scheme (OSMP7), based on the Lax-Wendroff approach to obtain a 7^{th}-order accurate coupled time and space approximation. A 2^{nd}-order centered scheme is used for the diffusive fluxes [2]. The ability of this code to compute high Reynolds compressible (turbulent and shocked) flows has already been demonstrated in a previous work [3].

3 Unsteady shock wave laminar boundary layer interaction (SWLBLI).

As a first step, by simulating the interaction between a laminar boundary layer and an incident shock wave, we suppress the suspected influence of the large turbulent structures of the boundary layer on the unsteadiness of the whole shock-wave/separation bubble system. The only remaining suspected cause of unsteadiness would be the dynamics of the separation bubble.
The flow conditions are similar to the test case of Degrez [5] ($M = 2.15$) with a shock wave angle increased up to $33.8°$ in order to strengthen the interaction and trigger the unsteadiness of the separation bubble.

The inlet boundary layer is created at the inlet of the domain thanks to a 4^{th} order polynomial approximation of a Blasius profile [10]. No-slip wall and adiabatic wall conditions are prescribed at the flat plate location ($y = 0$). Outlet time dependent non-reflecting boundary conditions [9]

are imposed at the top surface and at the downstream outlet boundary of the computational domain. Periodic conditions are used in the spanwise direction (z). The shock wave is created at the top boundary by using the Rankine-Hugoniot relationships.

The domain is discretized using a cartesian mesh with non uniform spacing in the direction normal to the wall (y). The mesh size employs $400 \times 102 \times 200$ grid points in $(x \times y \times z)$. In the normal to the wall direction, the mesh is tightened close to the wall using a hyperbolic tangent law.

Figure 1 shows a snapshot visualisation of the simulation consisting in isovalues of the Q criterion colored by the magnitude of the sreamwise velocity component. Shock waves are highlighted by isosurfaces of $div(\mathbf{u})$.

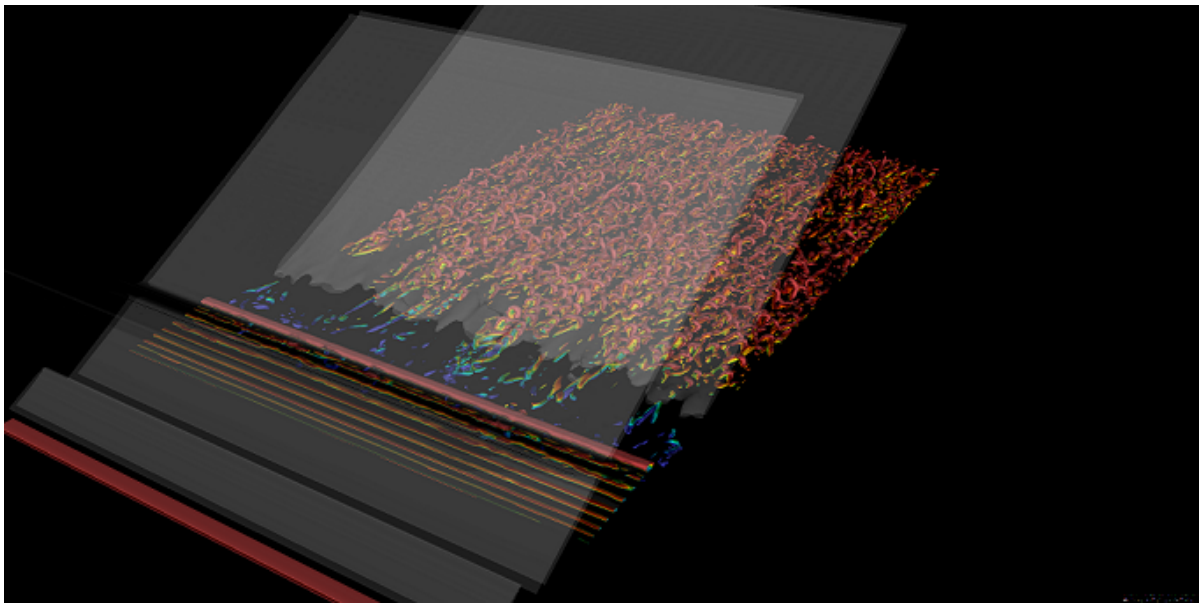

Figure 1 – Q criterion colored by longitudinal speed. Shock wave are highlighted by isosurfaces of $div(\mathbf{u})$.

First results have shown that the location of the reattachment point of the recirculation bubble have an oscillatory motion. It is clearly visible in the figure 2 where the history of the mean value in the spanwise direction of the reattachment point abscissa along the flate is plotted versus time.

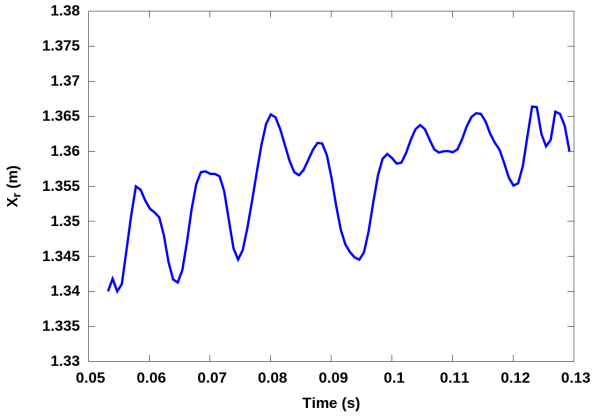

Figure 2 – History of the mean reattachment point abscissa in the spanwise direction along the flat plate.

A strong intermittency of the shedding responsible for low-frequency reattachment shock oscillations have also been evidenced. Nevertheless, in this configuration, the separation point of the recirculation bubble has a fixed location along the flat plate as shown in figure 3, where the history of the mean value in the spanwise direction of the separation point abscissa along the flat is plotted.

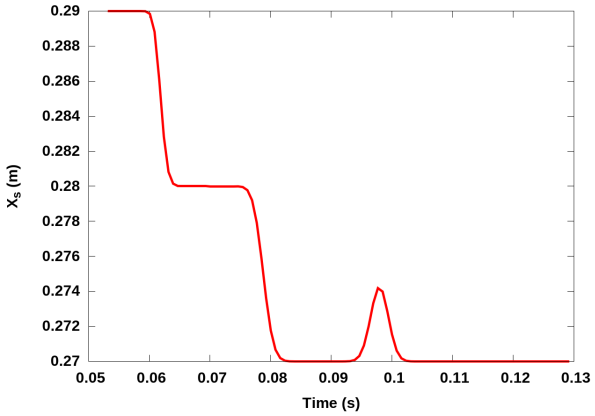

Figure 3 – History of the mean separation point abscissa in the spanwise direction along the flat plate.

Consequently, even if the recirculation bubble shows an unsteady motion, no unsteadiness of the whole SWBLI system occurs for this interaction with a laminar boundary layer. These first results suggest that the turbulent structures in the incoming boundary layer seem to have an impact on the low frequency oscillation of the SWBLI system.

4 Unsteady shock wave turbulent boundary layer Interaction (SWTBLI).

In this context, the accurate simulation of a turbulent compressible incoming boundary layer is of great importance. This is why a Synthetic Eddy Method [4] that we adapted to compressible

flows, has been developed to achieve this objective without prohibitive additional computational costs.

4.1 Simulation of the compressible turbulent boundary layer.

A compressible turbulent boundary layer have been simulated using the synthetic inlet conditions. The flow conditions ($M_\infty = 2.33$, $Re_\theta = 2538.78$) are taken from [11] where a method is developed to trip an incoming laminar boundary layer and to obtain a turbulent boundary layer. We employ $800 \times 320 \times 120$ grid points in $(x \times y \times z)$. In the normal to the wall direction, the mesh is tightened close to the wall using a hyperbolic tangent law to ensure that the first $y^+ = 0.8$. The domain extent is $60.4\delta \times 16.7\delta \times 3.0\delta$ where δ is the inlet boundary layer thickeness.
A snapshot (Q criterion colored by the longitudinal velocity) of the turbulent boundary layer obtained using this method is shown in figure 4.

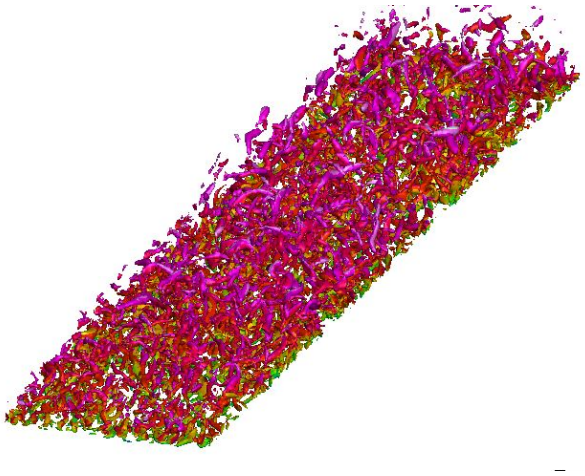

Figure 4 – Turbulent boundary layer : Q criterion colored by the longitudinal velocity.

The skin friction coefficient along the flat plate is plotted in figure 5. The adjustment distance needed to recover the right value of the skin friction coefficient is approximately $\Delta \sim 10\delta - 15\delta$. This adjustment distance appears to be very small compared to the one obtained by Mullenix and Gaitonde in [11].

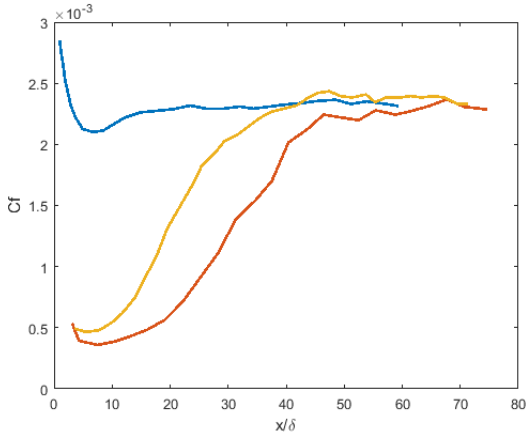

Figure 5 – Skin friction coefficient averaged in the spanwise direction along the flat plate. In blue, the DNS using synthetic eddy method. In red, result from [11] (coarse mesh). In yellow, result from [11] (fine mesh).

The diagonal components of the Reynolds stress tensor are also plotted on figure 6 with respect to the wall normal direction in wall units (y^+) for a fixed abscissa along the flat plate : $x = 30\delta$ (δ is the boundary layer thicknesses at the inlet). The distribution of the Reynolds stress tensor components above the flat plate are in good agreement with the reference values obtained from [11] with a different procedure.

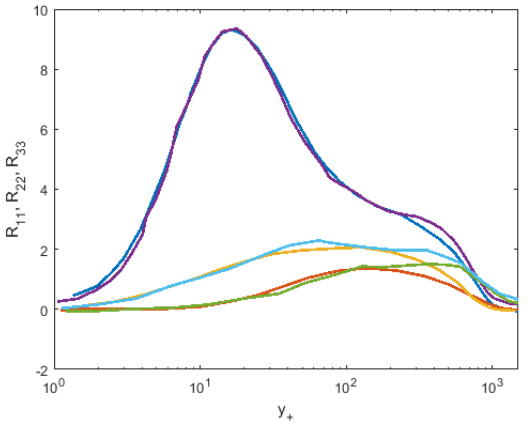

Figure 6 – Components of the Reynolds stress tensor (normalized using the friction velocity (u_τ) and the density at the wall (ρ_w)) with respect to the wall normal direction in wall units (y^+) : In blue, R_{11} obtained by DNS using synthetic eddy method for $x/\delta = 30$. In yellow, R_{33} obtained by DNS using synthetic eddy method for $x/\delta = 30$. In red, R_{22} obtained by DNS using synthetic eddy method for $x/\delta = 30$. In purple, R_{11} profile from [11] (fine mesh) for $x/\delta = 62.5$. In cyan, R_{33} profile from [11] (fine mesh) for $x/\delta = 62.5$. In green, R_{22} profile from [11] (fine mesh) for $x/\delta = 62.5$.

Finally, the Van-Driest streamwise mean velocity profile is plotted on figure 7. The velocity profile obtained corresponds to a turbulent profile with a linear evolution close to the wall, following by a log-law evolution in the inertial region with the right parameters.

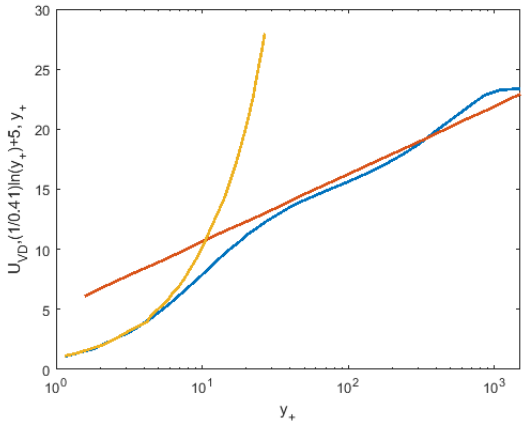

Figure 7 – Van Driest transform of the time averaged streamwise velocity versus y^+ for $x/\delta = 30$, logarithmic law ($\frac{1}{0.41}ln(y^+) + 5$) with respect to y^+ and the linear evolution in the inner layer.

These results show the ability of the Synthetic Eddy Method to accurately compute a compressible turbulent boundary layer. The adjustment distance is relatively short, shorter than other proposed procedures [11], which is very attractive in order to limit the streamwise extent of the computational domain and consequently the computational costs.

4.2 Simulation of the unsteady shock wave turbulent boundary layer interaction (SWTBLI)

In order to perform the simulation of the SWTBLI, an incident shock wave have been created on the top boundary layer using the Rankine-Hugoniot relashionships in the simulation of the compressible turbulent boundary layer presented in 4.1. This shock wave has an angle of 33.2° with respect to the longitudinal direction, as in [12] where a LES of a SWTBLI have been performed with the same flow conditions. The abscissa where the Rankine Hugoniot relationships are imposed on the top boundary layer is chosen so that the shock would impinges the flat plate at $x = 39.5.\delta$ in non-viscous flow, where δ is the boundary layer thickness prescribed at the inlet. As shown in 4.1, the turbulent boundary layer is well developed for this abscissa along the flat plate.

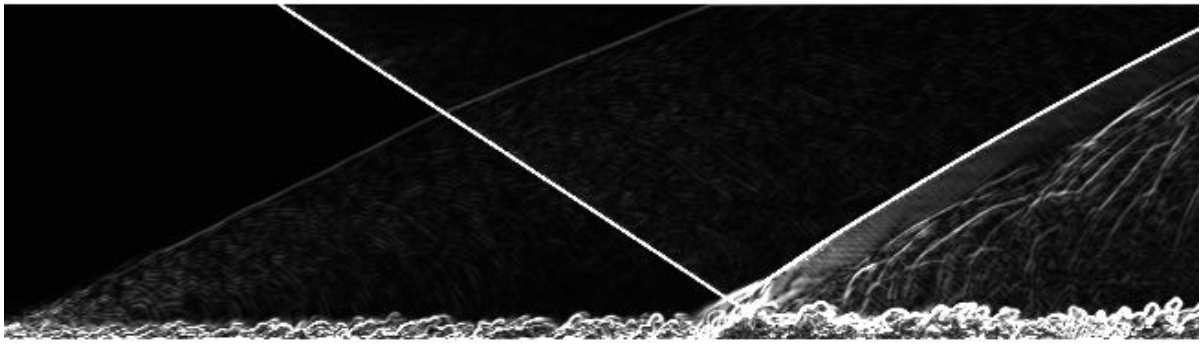

Figure 8 – Numerical schlieren visualization (2D slice located at the middle of the domain) obtained by plotting the norm of the density gradient ($||\nabla\rho||$).

A 2D slice located at the middle of the domain, of the numerical Shlieren have been plotted in figure 8. The characteristic properties of a SWTBLI have been recovered by our DNS. Indeed, we clearly see that the boundary layer thickness increases drastically due to the pressure rise imposed by the incident shock wave, leading to the creation of the reflected shock wave. The thickening of the boundary layer is also visible in figure 9 where the Q criterion isosurfaces have been plotted, colored by the magnitude of the spanwise velocity. The system of shocks have been evidenced by plotting isosurfaces of $\nabla \cdot \mathbf{u}$.

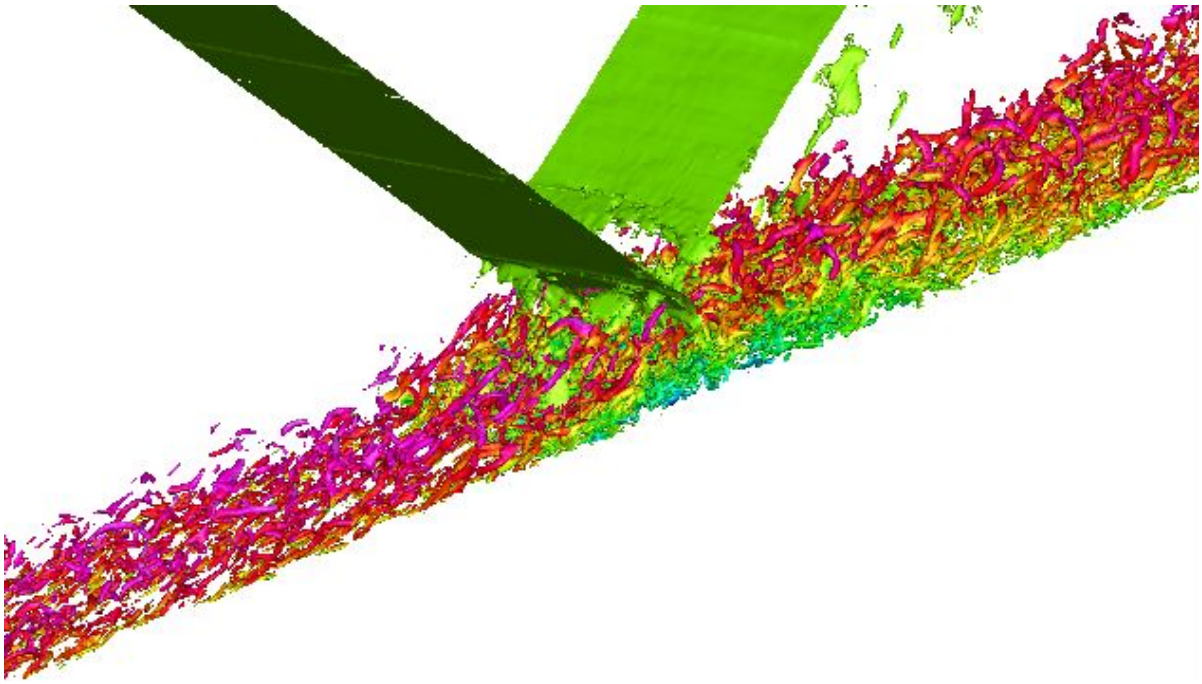

Figure 9 – Q criterion colored by the magnitude of the streamwise velocity. Shock waves are highlighted by isosurfaces of $div(\mathbf{u})$.

We see in figure 9 the presence of a region with low and negative streamwise velocity (colored in blue), located between the reflected and the incident shock waves. This separation bubble has a mean length $L_{sep} \sim 4.5\delta$ as shown in figure 10 where the time averaged skin friction coefficient along the flat plate, averaged in the spanwise direction, is plotted. This value of the separation length is in very good accordance with the one found in [12].

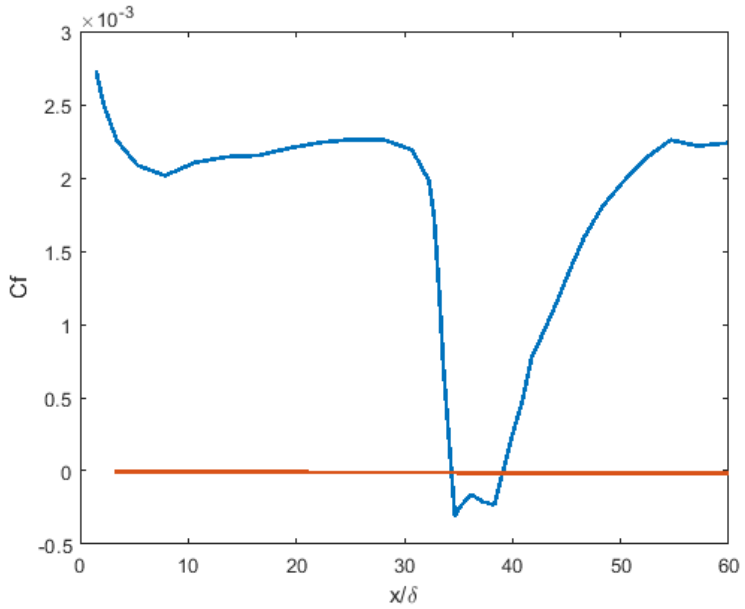

Figure 10 – Skin friction coefficient averaged in the spanwise direction along the flat plate. The red line indicates the zero value.

Further downstream of the separation, compression waves are visible in figure 8 due to the reattachment of the boundary layer.

As for the simulation of the SWLBLI, the history of the mean value in the spanwise direction of the separation and reattachment point abscissa along the flate have been plotted versus time in figures 11 and 12. We see in figure 12 that, as for the SWLBLI simulation, the reattachment point is submitted to an oscillatory motion. In the simulation of the SWLBLI, the position of the separation point had a fixed position along the flat plate. As shown in figure 11, the separation point is now submitted to an oscillatory motion when the incoming boundary layer is turbulent. Moreover, even if an accurate spectral analysis would not be succesfull because the separation point's history shown in figure 11 is plotted for a small time extent, we can visually identify the lower frequency contained is this signal about $f \simeq 1000Hz$ which can be nondimensionalized as $S_L = \frac{fL_{sep}}{U_e} \simeq 0.04$. This Strouhal number corresponds also to the frequency of the SWTBLI unsteadiness [1].

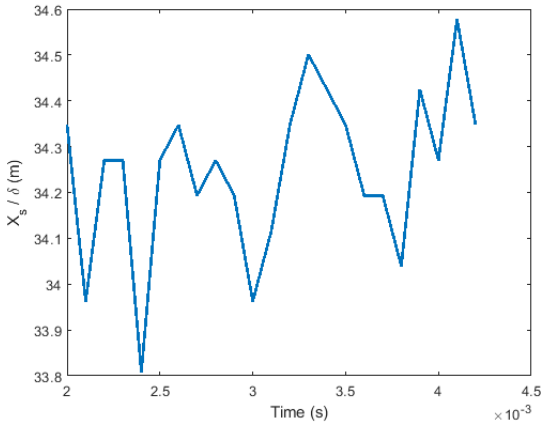

Figure 11 – History of the mean separation point abscissa in the spanwise direction along the flat plate.

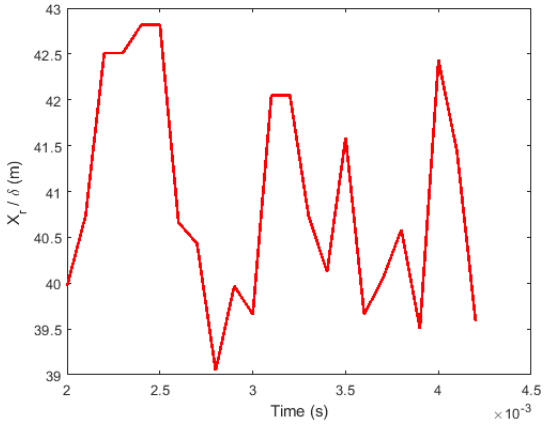

Figure 12 – History of the mean separation point abscissa in the spanwise direction along the flat plate.

The DNS of the SWTBLI using the Synthetic Eddy Method as inlet boundary conditions seems to be consistant with the known physical behavior of the SWTBLI and also with other simulations published by other authors. Indeed, the mean properties of the flow, as well as some caracteristic dynamic features (SWBLI unsteadiness) of the flow have been reproduced. The long term simulation of the SWTBLI (currently running) will allow us to acurately study the dynamics of the flow in order to better understand the onset of the SWTBLI unsteadiness.

5 Conclusion and prospect.

Simulations of the unsteady interaction of an incident oblique shock wave with a boundary layer developing on a flat plate have been performed by using a high-order shock capturing scheme to investigate the origin of the unsteadiness of the whole shock-waves/recirculation bubble system. First, an incoming laminar boundary layer has been considered. The unsteadiness of the reattachment shock was only found at a frequency in accordance with the flapping of the recirculation bubble but no unsteadiness of the whole system shock-waves/recirculation bubble

was recorded. These results show that the dynamics of the recirculation bubble (namely, the flapping, the shedding and the mixing layer unsteadinesses) [8, 7] is not the only mechanism responsible for the whole shock-waves/recirculation bubble unsteadiness. It is then obvious that the turbulent structures in the incoming boundary layer [6] take an important part in the low frequency motion of the shock-waves/recirculation bubble system.

Therefore, an incoming turbulent laminar boundary layer has secondly been considered. We adapted a Synthetic Eddy Method to the compressible regime for prescribing fluctuating inlet boundary conditions that are able to adjust a well established turbulent boundary layer in a reasonable streamwise extent and without a prohibitive additional computational cost. The DNS of a shock wave turbulent boundary layer interaction have then been preformed. Results are in good agreement with the literature. The mean extent of the detachment ($L_{sep} \sim 4.5\delta$) is in good accordance with previous studies [12]. Moreover, the SWTBLI unsteadiness have been recovered as the separation point have a low frequency oscillatory motion. This simulation is still running and probes have been placed in crucial locations in the flow field. The long term simulation of the flow will allow us to perform analyses of the flow dynamics in order to study the SWTBLI unsteadiness that will be presented at the conference. A comparison of the SWLBLI and SWTBLI dynamics will also be possible.

6 Acknowledgments.

This work has been performed using HPC resources from GENCI-IDRIS, France (Grant A0052A07195)

Références

[1] Delery, J. and Dussauge, J.-P. : Some physical aspects of shock wave/boundary layer interactions, Shock Waves, 19, 453–468 (2009).

[2] Daru, V. and Tenaud, C. : High Order One-step Monotonicity-Preserving Schemes for Unsteady Compressible flows Calculations, Journal of Computational Physics, 193, 563–594 (2004).

[3] Ben Hassan Saidi, I., Tenaud, C. and Fournier, G. : Solving three dimensional turbulent compressible flows using a high order One Step Monotony Preserving scheme, Proc. of Tenth International Conference on Computational Fluid Dynamics, July 9-13, Barcelona, Spain, (2018).

[4] Jarrin, N., Benhamadouche, S., urence, D. and Prosser, R. : A synthetic-eddy-method for generating inflow conditions for large-eddy simulations, Journal of Heat and Fluid Flow, 27, 585-593 (2004).

[5] Degrez, G., Boccadoro, C.H. and Wendt, J.F. : The interaction of an oblique shock wave with a laminar boundary layer revisited. An experimental and numerical study, Journal of fluid mechanics, 177, 247-263 (1987).

[6] Ganapathisubramani B., Clemens N. T. and Dolling D. S. : Planar imaging measurements to study the effect of spanwse structure of upstream turbulent boundary layer on shock-induced separation, AIAA Sciences Meeting and Exhibit, 44, 324 (2006).

[7] Aubard G., Gloerfelt X. and Robinet J.-C. : rge-Eddy Simulation of Broadband Unsteadiness in a Shock/Boundary-yer Interaction, AIAA Journal, 51, 2395-2409 (2013).

[8] Pirozzoli S. and Grasso F. : Direct Numerical Simulation of Impinging Shock Wave/Turbulent Boundary yer Interaction at M = 2.25, Physics of fluids, 18, 065113 (2006).

[9] Thompson K.W. : Time Dependent Boundary Conditions for Hyperbolic Systems, Journal of computational physics, 68, 1-24 (1987).

[10] Fournier G., Sellam M., Chpoun A., Fraigneau Y. and Tenaud C. : DNS of the interaction between an oblique shock wave and a boundary layer developing along a flat plate, , , (2018).

[11] Mullenix N. J. and Gaitonde D. V. : Spatially Developing Supersonic Turbulent Boundary yer with a Body-Force-Based Method, AIAA Journal, 51, 1805-1819 (2013).

[12] Adler M. C. and Gaitonde D. V. : Dynamic linear response of a shock/turbulent-boundary-layer interaction using constrained perturbations, J. Fluid Mech., 840, 291-341 (2018).